Vibrational Analysis of Amino Acids and Short Peptides in Hydrated Media. I. L-glycine and L-leucine

ARTICLE *in* THE JOURNAL OF PHYSICAL CHEMISTRY B · MARCH 2007

Impact Factor: 3.3 · DOI: 10.1021/jp0633953 · Source: PubMed

Vibrational Analysis of Amino Acids and Short Peptides in Hydrated Media. I. L-glycine and L-leucine

Najoua Derbel,[†] Belén Hernández,[‡] Fernando Pflüger,[‡] Jean Liquier,[‡] Frédéric Geinguenaud,[‡] Nejmeddine Jaïdane,[†] Zohra Ben Lakhdar,[†] and Mahmoud Ghomi*[,‡]

Laboratoire de Spectroscopie Atomique Moléculaire et Applications (LASMA), Département de Physique, Faculté des Sciences de Tunis, Campus Universitaire, 2092 EL MANAR II, Tunisia, and Laboratoire de Biophysique Moléculaire, Cellulaire et Tissulaire (BioMoCeTi), UMR CNRS 7033, UFR SMBH, Université Paris 13, 74 rue Marcel Cachin, 93017 Bobigny cedex, France and Université Pierre et Marie Curie, Case 138, 4 Place Jussieu, 75252 Paris cedex 05, France

Received: June 1, 2006; In Final Form: December 8, 2006

Raman scattering and Fourier-transform infrared (FT−IR) attenuated transmission reflectance (ATR) spectra of two α-amino acids (α-AAs), i.e., glycine and leucine, were measured in H_2O and D_2O (at neutral pH and pD). This series of observed vibrational data gave us the opportunity to analyze vibrational features of both AAs in hydrated media by density functional theory (DFT) calculations at the B3LYP/6-31++G* level. Harmonic vibrational modes calculated after geometry optimization on the clusters containing each AA and 12 surrounding water molecules, which represent primary models for hydration scheme of amino acids, allowed us to assign the main observed peaks.

I. Introduction

The behavior of amino acids (AAs) in aqueous solutions is of a major interest because water is the natural medium for biological molecules. A detailed knowledge of AA interactions with water is a primary step in understanding the solvation process of larger systems, such as peptides and proteins. Hydrophilic or hydrophobic feature of the side chain (R) also plays an important role in the hydration process of a given amino acid. Geometric and hydration analyses of glycine (G), considered as a prototype for larger AAs in both neutral and zwitterionic forms, have received considerable attention. Experimentally, in the context of mass spectrometric and size-selected photoelectron spectroscopic studies, it has been shown that five water molecules are needed to transform neutral glycine into its zwitterion.[1] Theoretically, one can recall here the first report presented by Clementi's group[2] in which an amino acid and a water molecule (W) were treated separately at the SCF level of theory, whereas their mutual interaction was considered by the use of a classical Buckingham potential. Since 10 years ago, a series of ab initio calculations have been devoted to the estimation of the relative stability of glycine conformers in gas and hydrated phases.[3−14] One of these reports considers the glycine environment (including water) as a dielectric continuum characterized by its macroscopic permittivity.[9] In other reports, HF, DFT/B3LYP and MP2 methods have been applied to study the complexation of glycine with one water (referred to as G+1W) cluster molecule placed differently around this amino acid.[7,10−11] The whole geometry was optimized by means of different Gaussian basis sets and the relative stability of 1:1 complex (G+1W) configurations was estimated. It was concluded that the geometrical data obtained at the DFT and MP2 levels are more reliable than those estimated at the HF level even when extended basis sets are used. Zwitterionic form of the G+1W cluster was shown to be unstable, and the geometry optimization tends in all cases toward a neutral form of G. Moreover, the vibrational wavenumbers calculated at the DFT level on an isolated G (neutral form) have been compared with those observed in the gas phase without the use of any scaling factor thanks to a good agreement between experimental and theoretical data.[11] A systematic theoretical analysis at the DFT/B3LYP/6-31++G** level supported by experimental matrix-isolation FT−IR results,[12] pointed to the necessity of at least two water molecules to maintain the zwitterionic form, thus avoiding the proton transfer from NH_3^+ to COO^- group upon geometry optimization. However, the zwitterionic G+2W and G+3W were found to be less stable than neutral forms of the same complexes. For G+4W and G+5W complexes, the higher stability of the zwitterionic forms was proved. We must emphasize two recent systematic theoretical works devoted to the tautomerization (zwitterionic → neutral form) of isolated and hydrated G.[13−14] Different clusters containing a number of water molecules varying from one to six were considered in the mentioned calculations performed at the DFT/B3LYP level with the basis sets equipped with diffuse functions at least on heavy atoms. It has been again confirmed, as reported in other works (see above), that the neutral species exist in the gas phase as well as in mono- and dihydrated clusters, whereas for a larger number of water molecules, the zwitterionic form is better solvated than the neutral one. Thus, the zwitterion to neutral tautomerization becomes less exothermic for clusters containing up to three water molecules and endothermic for larger clusters, and the neutral form does not exist for some solvent arrangements with five water molecules. In addition to all theoretical reports mentioned above, which have given a static picture of hydrated glycine and its proton-transfer mediated or not by water molecules, a recent work has proposed a very interesting

* Corresponding author phone: +33-1-48387351 or +33-1-169874354; fax: +33-1-48387356 or +33-1-169874360. e-mail: ghomi@smbh.univ-paris13.fr or ghomi@ccr.jussieu.fr.

[†] Campus Universitaire El Manar.

[‡] Université Paris 13 and Université Pierre et Marie Curie.

10.1021/jp0633953 CCC: $37.00
Published on Web 01/23/2007

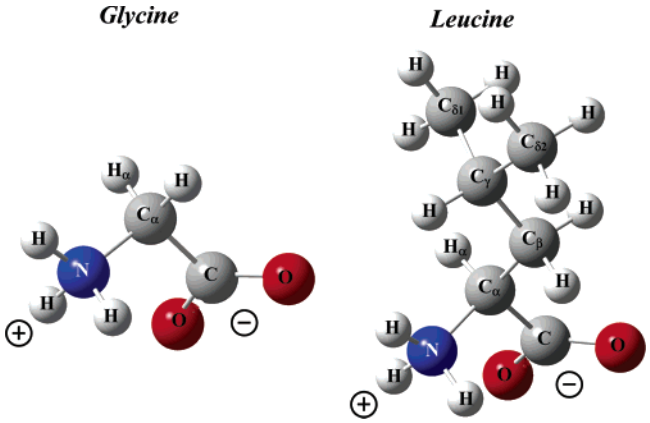

Figure 1. Chemical structures of glycine (left) and leucine (right).

dynamic representation of these aspects by means of a combined use of QM/MM and ab initio Car−Parrinello molecular dynamics (CPMD).[15] Fundamental questions have been addressed through the results obtained over a 10−20 ps dynamics, such as (i) energy barriers for proton transfer, (ii) time-dependent hydration numbers on COO^- and $NH3^+$ groups, and (iii) pair-correlation functions between the oxygen, nitrogen and hydrogen atoms of glycine and hydrogen atoms on water molecules. As far as the G hydration is concerned, the conclusion of this extensive work was that 4.7 water molecules are bound in average to COO^- group, whereas 3.0 hydrogen bonds are predicted between the NH_3^+ group and water molecules. Despite the above-mentioned careful analyses on G hydration, a theoretical investigation of its vibrational properties in hydrated media is still lacking in the literature. This is also the case for most of the AAs. The only data available on the assignment of AA vibrational modes (and those arising from side chains: 1400−1200 cm^{-1} region) are based on the isotopic shifts observed in aqueous solution Raman spectra of native and deuterated species (deuteration on C_α as well as on the carbons of their side chains) in some AAs with nonaromatic and aromatic side chains.[16−18]

The present work reports the first part of a series of our investigations devoted to the analysis of vibrational properties of amino acids and short peptides in hydrated media. Here, our attention is basically focused on the vibrational features of two AAs: glycine (G) with R = H, the structurally simplest AA, and leucine (L) with a large size hydrophobic side chain, R = CH_2−CH-$(CH_3)_2$ (Figure 1). From the experimental point of view, we present newly recorded Raman spectra of both AAs complimented by their FT−IR spectra recorded in H_2O and D_2O. In order to propose theoretical results based on the models which permit comparison with experiments, we have undertaken vibrational calculations at the DFT/B3LYP level on the clusters containing 12 water molecules mimicking reasonably the hydration scheme in the vicinity of glycine and leucine backbone.

II. Experimental Details

Powder samples of the AAs were purchased from Calbochem and Sigma-Aldrich and used as provided. Solutions of both AAs were prepared by dissolving each compound in phosphate buffer, pH (pD) = 6.8, containing 10 mM monovalent cations (Na^+ and K^+) and 1 mM EDTA, to obtain aqueous samples of 50 mM molecular concentration used for Raman spectroscopy. FT−IR (ATR) spectra were obtained from solutions of AAs (c = 100 mM) prepared directly in H_2O or D_2O. Raman spectra were excited at 488 nm with an Ar^+ laser (Stabilite model 2017-04S, Spectra Physics) and collected on a Jobin-Yvon T64000 spectrograph in a single spectrograph configuration with a 1200 grooves/mm holographic grating and a holographic notch filter. The spectrograph is equipped with a liquid nitrogen cooled CCD detection system (Spectrum One, Jobin-Yvon) based on a Tektronix CCD chip of 2000 × 800 pixels. The effective spectral slit width was set to ca. 5 cm^{-1}. Raman spectra were collected at room temperature. ATR spectra of AAs were recorded at room temperature with a FT−IR Perkin-Elmer 2000 spectrophotometer equipped with an ATR accessory, under continuous dry air purge. Solutions in D_2O (>99.8%) purity, purchased from Euriso-Top CEA), were prepared under dry air atmosphere. Typically 18 μL of sample solutions were deposed in drops on the ZnSe crystal of the ATR accessory, and spread to cover the whole surface. Infrared beam, with an effective angle of incidence of 45°, follows 12 reflections from the entrance to the exit points in the ATR crystal. The effective path length (number of reflections × depth of penetration, dp) was around 15 micrometers, where dp is calculated as follows: $dp = (\lambda/n_c)/(2\pi[\sin^2\theta - (n_s/n_c)^2]^{1/2})$, where λ = wavelength (mm), n_c = refractive index of crystal, n_s = refractive index of sample, θ = crystal face angle (degrees). Usually 20 scans were collected with 1 cm^{-1} spectral resolution and a medium Norton Beer apodization function. Postprocessing (subtraction of buffer contribution, baseline correction and smoothing) of Raman spectra was performed using GRAMS/32 software (Galactic Industries). ATR data treatment was performed using the Perkin-Elmer Spectrum program and consisted only in solvent subtraction and multiple-point baseline correction. Final presentation of vibrational spectra shown in this paper has been performed by means of SIGMAPLOT package.

III. Theoretical Details

To analyze the geometrical and vibrational features of AAs with their surrounding water molecules, the DFT method has been adopted because of its excellent compromise between computational cost and involvement of electronic correlation. All quantum mechanical computations have been performed on the IBM workstations using the GAUSSIAN03 package.[19] B3LYP functional, with Becke's three parameter (B3) exchange functional,[20] along with the Lee−Yang−Parr (LYP) non local correlation functional,[21] were used. Split valence double-ζ gaussian atomic basis sets containing diffuse functions on both heavy and hydrogen atoms, i.e., 6-31++G*, were employed in order to give a static picture of zwitterionic character of amino acids in aqueous medium by taking into account the results obtained by previous static DFT calculations on penta- and hexa-hydrated glycine,[14] as well as those of recent CPMD calculations.[15] To achieve this objective, geometry optimization was first carried out on a simple model G+3W. As shown in previous works,[11−14] the presence of three water molecules, placed between COO^- and NH_3^+ chemical groups and forming intermolecular H-bonds: W···W and W···AA, is absolutely necessary to avoid proton transfer between the two charged sides of G. In further steps, we have considered a total number of 12 water molecules in order to fully hydrate COO^- (4 W) and $NH3^+$ groups (3 W) and to create a reasonable hydrogen bond network between their hydration shells. Optimized structure of G+12W was considered as a starting point for modeling hydrated leucine. We have replaced the glycine side chain by that of leucine (Figure 1). No additional water molecule was placed around the L side chain because of its hydrophobic character. The whole cluster L+12W was then geometry optimized. No correction due to the basis set superposition error

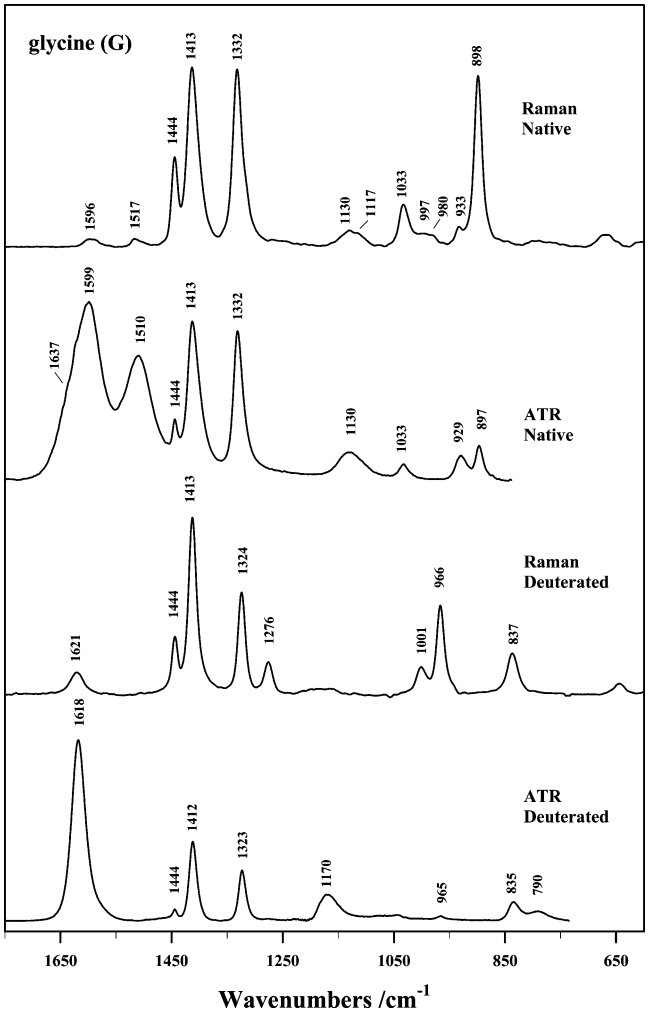

Figure 2. Vibrational spectra of glycine observed in aqueous solutions. From top to bottom: Raman spectrum recorded in H_2O buffer (λ_L = 488 nm), FT−IR ATR spectrum recorded in H_2O buffer, Raman spectrum recorded in D_2O (λ_L=488 nm), FT−IR ATR spectrum recorded in D_2O. The intensity of each observed spectrum was normalized to the most intense peak in order to facilitate their comparison.

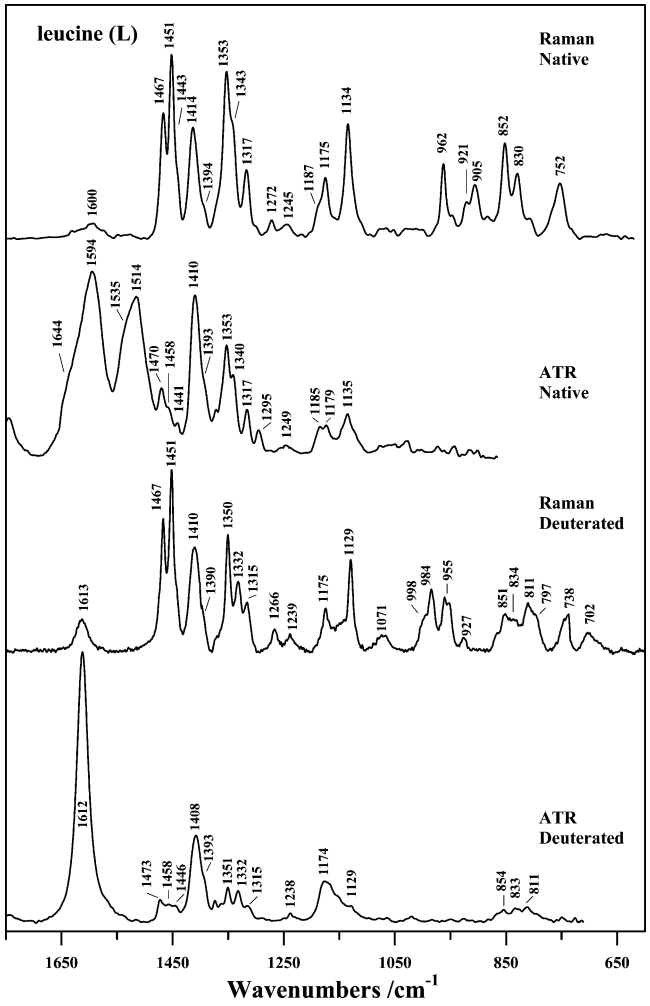

Figure 3. Vibrational spectra of leucine observed in aqueous solutions. From top to bottom: Raman spectrum recorded in H_2O buffer (λ_L = 488 nm), FT−IR ATR spectrum recorded in H_2O buffer, Raman spectrum recorded in D_2O (λ_L = 488 nm), FT−IR ATR spectrum recorded in D_2O. The intensity of each observed spectrum was normalized to the most intense peak in order to facilitate their comparison.

(BSSE) was considered in the course of quantum mechanical calculations. As shown in our previous calculations on hydrated uracil at the same level of theory the BSSE correction brings only a negligible change to electronic energy.[22] Harmonic vibrational calculations performed after full geometry optimization provided no imaginary frequency, leading to conclude that G+12W and L+12W optimized geometries correspond well to local energy minima. Hessian matrix containing cartesian force constants, output from the Gaussian package, was post-treated by means of a homemade program (BORNS) allowing us to remove redundancies among vibrational coordinates and to assign wavenumbers on the basis of the PED (potential energy distribution) matrix elements as expressed in terms of a combination of local symmetry and internal coordinates (atomic cartesian coordinates of the optimized geometries, cartesian force constants and assignments of all calculated wavenumbers are available upon request). Local symmetry coordinates are those generally defined in the case of perfect C_{2v} and C_{3v} point groups; they reflect the symmetric or antisymmetric character of corresponding vibrations. However, we are conscious that the local C_{2v} (for COO^- and CH_2) or C_{3v} (NH_3^+ and CH_3) symmetries are lowered when the corresponding chemical groups are introduced in the backbone or the side chain of AAs.

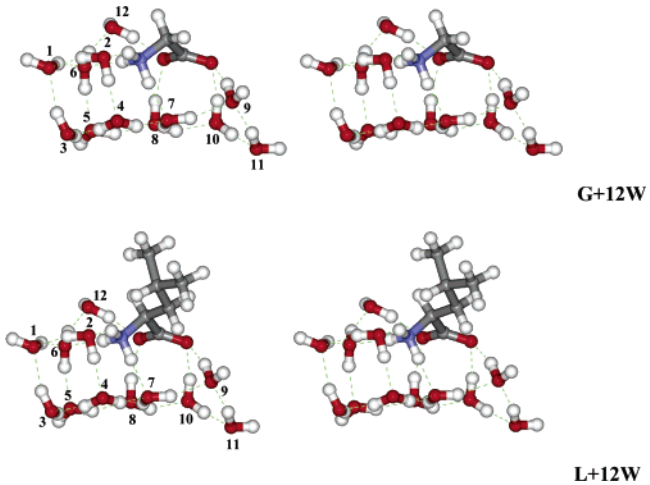

Figure 4. Stereoviews of G+12W (top) and L+12W (bottom) supermolecules. Geometry optimization was performed at the DFT/B3LYP/6-31++G* level of theory. Water molecules are numbered from 1 to 12 on the left part of each Figure.

The whole AA (with or without its surrounding water molecules) possesses evidently a global C_1 symmetry. This explains the

TABLE 1: Energetics and Most Prominent Geometrical Parameters of Glycine (G) and Leucine (L) as Obtained from the Theoretical Optimized with 12 Surrounding Water (W) Molecules[a]

energies	G + 12W	L + 12W
E_e	−1201.747536	−1359.008581
E_v	245.207	316.301

bond lengths	G + 12W	L + 12W	bond lengths	L + 12W
N-H1	1.040	1.040	Cβ-H1	1.098
N-H2	1.056	1.053	Cβ-H2	1.097
N-H3	1.046	1.046	Cβ-Cγ	1.546
N−Cα	1.494	1.508	Cγ-H	1.099
Cα-Hα	1.093	1.094	Cγ-Cδ1	1.538
Cα-C	1.548	1.560	Cγ-Cδ2	1.538
C-O1	1.267	1.270	Cδ1-H1	1.096
C-O2	1.256	1.254	Cδ1-H2	1.096
Cα-H (−Cβ)	1.091	1.528	Cδ1-H3	1.099
			Cδ2-H1	1.096
			Cδ2-H2	1.099
			Cδ2-H3	1.097

valence angles	G + 12W	L + 12W	valence angles	L + 12W	valence angles	L + 12W
H1-N-H2	106.17	105.60	Cα-Cβ-H1	108.56	H1-Cδ1-H2	107.05
H1-N-H3	107.18	106.97	Cα-Cβ-H2	107.25	H1-Cδ1-H3	107.75
H2-N-H3	105.73	105.91	Cα-Cβ-Cγ	116.11	H2-Cδ1-H3	107.66
H1-N−Cα	112.13	111.78	Cβ-Cγ-H	109.11	Cγ-Cδ2-H1	110.97
H2-N−Cα	116.30	116.43	Cβ-Cγ-Cδ1	112.36	Cγ-Cδ2-H2	111.01
H3-N−Cα	108.80	109.58	Cβ-Cγ-Cδ2	109.48	Cγ-Cδ2-H3	111.46
N−Cα-H (−Cβ)	108.38	111.01	H1-Cβ-H2	106.06	H1-Cδ2-H2	107.69
N−Cα-Hα	108.60	106.34	Cγ-Cβ-H1	109.17	H1-Cδ2-H3	107.59
N−Cα-C	107.97	105.02	Cγ-Cβ-H2	109.23	H2-Cδ2-H3	107.95
H(Cβ-)-Cα-C	111.75	115.67	Cδ1-Cγ-H	108.13		
Hα-Cα-C	110.54	107.28	Cδ1-Cγ-Cδ2	110.38		
H(Cβ-)-Cα-H	109.50	110.95	H−Cγ-Cδ2	107.23		
Cα-C-O1	115.15	114.46	Cγ-Cδ1-H1	112.71		
Cα-C-O2	118.75	119.96	Cγ-Cδ1-H2	110.51		
O1-C-O2	125.98	125.46	Cγ-Cδ1-H3	110.94		

water molecules	G + 12W	L + 12W	water molecules	G + 12W	L + 12W
W1(O-H1)	0.969	0.969	W7(O-H1)	0.988	0.989
W1(O-H2)	0.989	0.990	W7(O-H2)	0.982	0.981
W1(H−O−H)	107.33	107.37	W7(H−O−H)	106.21	105.97
W2(O-H1)	0.979	0.979	W8(O-H1)	0.987	0.988
W2(O-H2)	0.993	0.993	W8(O-H2)	0.996	0.996
W2(H−O−H)	104.27	104.18	W8(H−O−H)	100.92	100.84
W3(O-H1)	0.977	0.977	W9(O-H1)	0.997	0.996
W3(O-H2)	0.979	0.979	W9(O-H2)	0.969	0.969
W3(H−O−H)	105.57	105.49	W9(H−O−H)	107.48	107.19
W4(O-H1)	0.987	0.987	W10(O-H1)	0.978	0.978
W4(O-H2)	0.976	0.977	W10(O-H2)	0.984	0.984
W4(H−O−H)	104.53	104.60	W10(H−O−H)	104.84	104.92
W5(O-H1)	0.969	0.969	W11(O-H1)	0.982	0.983
W5(O-H2)	0.993	0.994	W11(O-H2)	0.968	0.968
W5(H−O−H)	106.64	106.70	W11(H−O−H)	106.79	106.77
W6(O-H1)	0.990	0.990	W12(O-H1)	0.968	0.968
W6(O-H2)	0.985	0.985	W12(O-H2)	0.991	0.992
W6(H−O−H)	107.31	107.43	W12(H−O−H)	107.16	107.12

H-bonds	G + 12W	L + 12W	H-bonds	G + 12W	L + 12W
W2(O)...HN	1.726	1.753	W9(H)...O−C	1.711	1.718
W6(O)...HN	1.894	1.903	W12(H)...O−C	1.746	1.733
W8(O)...HN	3.219	3.249	W8(H)...O−C	1.832	1.812
			W10(H)...O−C	2.173	2.203

[a] For atom numbering and chemical structures, see Figure 1. Optimized geometries are displayed in Figure 4. Bond lengths are in angstroms and valence angles in degrees.

coexistence of the symmetrical coordinates (belonging originally to different irreducible representations of C_{2v} or C_{3v} groups) in the PED of some vibrational modes. To take into account the AA···W and W···W H-bond interactions, additional internal coordinates such as X···H stretch (where X is a H-bond acceptor), AX···H and X···HY valence angles (where A and Y are the atoms covalently connected to the X and H atoms respectively), and AX···HY torsional coordinates are defined. No scaling factor has been applied to calculated vibrational wavenumbers because we preferred here a straightforward

TABLE 2: Assignment of the Glycine Vibrational Modes Observed in Aqueous Solutions[a]

glycine				glycine-deuterated			
Raman	IR	calc	assignment (PED%)	Raman	IR	calc	assignment (PED%)
	1637 (sh)	1773	NH3-asym bend (37); W2...NH3 (14); W6...N-H3 (12)				
1517 (w)	1510 (s)	1662	NH3-sym bend (27); NH3-sym rock (23); W12(H−O−H) (10); W2...NH3 (9)				
1596 (w)	1599 (s)	1650	COO^-asym st (60)	1621 (w)	1618 (s)	1665	COO^- asym st (85)
1444 (s)	1444 (m)	1510	Hα-Cα-H (79); N−Cα-Hα (8)	1444 (m)	1444 (w)	1510	Hα-Cα-H (79); N−Cα-Hα (8)
1413 (s)	1413 (s)	1430	COO^-sym st (51); Cα-C (14)	1413 (s)	1412 (m)	1427	COO^- sym st (58); Cα-C (14)
1332 (s)	1332 (s)	1373	N−Cα-H (30); NH3-asym rock (18); NH3-asym rock (15); N−Cα-Hα (9)				
		1363	N−Cα-Hα (27); COO^- sym st (20); Hα-Cα-C (16); NH3-asym rock (11); H−Cα-C (11)				
				1324 (s)	1323 (m)	1350	H−Cα-C (21); Hα-Cα-C (19); N−Cα-Hα (18); N−Cα-H (17); COO^- sym st (15)
				1276 (s)		1285	N−Ca-Ha (20); N−Ca-H (18)
					1170 (m)	1263	ND3-asym bend (14); ND3-sym bend(13); ND3-sym rock(11); W2... ND3 (11)
						1259	ND3-asym bend (27); W6...ND3(17); W2... ND3 (11); N−Cα-H (9)
1130 (m)	1130 (m)	1172	H−Cα-C (25); W2...NH3 (17); NH3-asym rock (12); N−Cα-C (10); W8...NH3 (10)				
1117 (m)		1148	NH3-asym rock (27); Hα-Cα-C (27); H−Cα-C (11); N−Cα-Hα (8)				
						1067	H−Cα-C (42); Hα-Cα-C (25); ND3-asym rock (14)
1033 (m)	1033 (w)	1022	N−Cα (75)				
				1001 (w)		1009	N−Cα (43); N−Cα-C (21)
997 (sh)		994	W8...O−C (34); W6...W12 (12); W5...W7 (9); W8...NH3 (8)				
980 (w)		973	W9...O−C (23); W6...W12 (18)				
				966 (m)	965 (w)	959	Cα-C (29); N−Cα (19); COO^- sym st (9)
933 (w)	929 (m)	943	W9...O−C (23)				
898 (s)	897 (m)	892	Cα-C (25); OCO (14); W8...NH3 (12); W7...W8 (11); COO^- sym st (10)				
				837 (m)	835 (w)	842	OCO (18); ND3-asym rock (17); $C\alpha COO^-$ sym bend (10); W2... ND3 (10); N−Cα(9)
					790 (sh)	830	ND3-asym rock (36); N−Cα-H (12); τ(Cα-C) (11); W8... ND3 (8)

[a] s. intense, m. medium, w. weak, sh. shoulder. Raman**:** vibrational wavenumbers in Raman spectra recorded in H_2O and D_2O buffers (Figure 2). IR: vibrational wavenumbers observed in FT−IR ATR spectra recorded in H_2O and D_2O (Figure 2). Calc: calculated results obtained at DFT/B3LYP/6-31++G* the level on a theoretical model including glycine surrounded by 12 water molecules (Figure 4). Only major contributions (PED ≥ 8%) are reported in this Table. Assignments of the vibrational modes are based on the potential energy distribution (PED) based on internal coordinates. In front of each internal coordinate is reported the corresponding PED (in percent).

comparison between observed wavenumbers and "raw" calculated ones in order to evidence the defaults of both the theoretical level (even though it is adequately chosen in the present work) and the harmonic approximation. The assignment of vibrational modes was undertaken by considering mainly their isotopic shifts. Particularly in the case of leucine, we have taken into consideration the assignments based on the vibrational spectra of alanine,[23−26] valine,[27] and leucine,[16] i.e., three amino acids with nonaromatic side chains.

IV. Results

Raman and FT−IR ATR Spectra. The observed vibrational spectra of glycine and leucine are displayed in Figures 2 and 3, respectively. In each Figure, we report the Raman and FT−IR spectra recorded in H_2O and D_2O buffers, each one normalized to its most intense band. The peak positions and spectral shape of Raman spectra in H_2O are very close to those reported previously.[23] In Tables 2 and 3 the wavenumbers and the relative intensities of the main peaks observed in each spectrum, are listed. Spectra recorded in D_2O buffer clearly show the effect of $NH_3^+ \rightarrow ND_3^+$, i.e., labile hydrogen deuteration, on the vibrational modes of each AA.

Theoretical Results. Stereoviews of optimized G+12W and L+12W clusters are shown in Figure 4, along with the numbering of water molecules. As it can be seen, among the twelve surrounding water molecules, eight are located at one side and the other four at the other side of the backbone of each amino acid. Six of the eight water molecules are located approximately in an average plane (W3, W4, W5, W7, W8, W10), at the same side of the backbone. Based on the present calculations, eight of the 12 water molecules are located undoubtedly in the first hydration shells of the backbone of each AA. The other four water molecules belong to the second shell of hydration (W1, W3, W5, W11), making intermolecular H-bonds with the water molecules of the first hydration shell. Table 1 shows the values of electronic (E_e) and vibrational

TABLE 3: Assignment of the Leucine Vibrational Modes Observed in Aqueous Solutions[a]

leucine				leucine-deuterated			
Raman	IR	calc	assignment (PED%)	Raman	IR	calc	assignment (PED%)
	1644 (sh)	1785	NH3-asym bend (23); W4(H−O−H) (13); W8(H−O−H) (10); W3...W4 (8)				
	1535 (sh)	1771	NH3-asym bend (44); W2...NH3 (10); W6...N-H3 (8)				
	1514 (s)	1652	NH3-sym bend (28); NH3 sym rock (23); COO^- asym st (10); W2...NH3 (8)				
1600 (w)	1594 (s)	1643	COO^- asym st (60)	1613 (m)	1612 (s)	1657	COO^- asym st (85)
	1470 (m)	1535	Cδ1-asym bend (54); Cδ2-asym bend (29)		1473 (w)	1535	Cδ1-asym bend (54); Cδ2-asym bend (30)
1467 (s)		1527	Cδ2-asym bend (43); Cδ1-asym bend (39)	1467 (s)		1527	Cδ2-asym bend (44); Cδ1-asymbend (38)
	1458 (sh)	1520	Cδ2-asym bend (49); Cδ1-asym bend (33)		1458 (w)	1520	Cδ2-asym bend (48); Cδ1-asym bend (34)
1451 (s)		1511	Cδ1-asym bend (40); Cδ2-asym bend (34); Cβ-bend (14)	1451 (s)		1511	Cδ1-asym bend (40); Cδ2-asym bend (34); Cβ-bend (16)
1443 (sh)		1501	Cβ-bend (72); Cδ1-asym bend (9)		1446 (w)	1502	Cβ-bend (70); Cd1-asym bend (10); Cd2-asymbend (8)
	1441 (w)	1446	Cδ2-sym bend (27); Cδ2-sym rock (24); Cδ1-sym bend (22); Cδ1-sym rock (19)	1443 (sh)		1446	Cδ2-sym bend (27); Cδ2-sym rock (24); Cδ1-sym bend (22); Cδ1-sym rock (19)
1394 (sh)	1393 (sh)	1427	Cδ1-sym bend (24); Cδ1-sym rock (21); Cδ2-sym bend (15); Cδ2-sym rock (14)	1390 (sh)	1393 (sh)	1427	Cδ1-sym bend (25); Cδ1-sym rock (22); Cδ2-sym bend (19); Cδ2-sym rock (17)
		1421	Cβ-rock (23); Cβ-Cα-Hα (14); N−Cα-Hα (11)			1417	COO^- sym st (23); Cβ-rock (20); Cβ-Cγ-H (8);
1414 (s)	1410 (s)	1417	COO^- sym st (49); N−Ca-Ha (11); Ca-C (10)	1410 (s)	1408 (m)	1412	COO^- sym st (37); Cβ-rock (12)
1353 (s)	1353 (s)	1402	Cβ-Cγ-H (31); Cβ-twist (10); N−Cα-Hα (10); Cδ1-Cγ-H (9)	1350 (s)	1351 (w)	1399	Cβ-Cγ-H (27); Cβ-twist (19); Cδ1-Cγ-H (17); Cβ-Cα-Hα (11); N−Cα-Hα (8)
1343 (sh)	1340 (sh)	1385	Cδ1-Cγ-H (24); Cδ2-Cγ-H (12); N−Cα-Hα (11); Cβ-rock (11)	1332 (s)	1332 (w)	1373	Cδ2-Cγ-H (27); Cδ1-Cγ-H (24); N−Cα-H (13); Cβ-Cα-Hα (10)
1317 (s)	1317 (m)	1359	Cδ2-Cγ-H (28); Cb-rock (11); Hα-Cα-C (9)	1315 (s)	1315 (w)	1350	Cβ-rock (24); N−Cα-Hα (22); Cδ2-Cγ-H (14); Hα-Cα-C (10)
	1295 (m)	1316	Cβ-twist (40); NH3-asym rock (9)				
1272 (m)		1288	Hα-Cα-C (27); Cβ-rock (27); NH3-asym rock (8)	1266 (m)		1297	Cβ-twist (25); Hα-Cα-C (8)
1245 (m)	1249 (w)	1226	Cδ1-asym rock (13); NH3-asym rock (12); Cβ-wag (11); Cβ-Cα-Hα (8)	1239 (m)	1238 (w)	1200	Cδ1-asym rock(24); Cδ2-asym rock (21); Cδ1-Cg-Cd2 (10)
						1266	ND3-asym bend (20)
						1262	ND3-asym bend (31); W6...ND3 (15)
						1252	ND3-sym bend (20); ND3-sym rock (17); ND3-asym bend (14); W2...ND3 (8)
1187 (sh)	1185 (m)	1198	Cδ1-asym rock (23); Cβ-Cγ(13); Cδ2-asym rock (11); Cδ2-asym rock (10)				
1175 (s)	1179 (m)	1176	H−Cα-C (16); NH3-asym rock (14); W2...NH3 (13); Cα-Cβ (10); N−Cα-C (10)	1175 (m)	1174 (m)	1180	Cβ-wag (19); Cδ1-asym rock (15); Cβ-Cg (9); Cα-Cβ (8)
1134 (s)	1135 (m)	1153	Cδ2-asym rock(17); Cγ-Cδ2 (11)	1129 (s)	1129 (sh)	1151	Cδ2-asym rock (17); Cγ-Cδ2 (13); Cγ-Cδ1 (9);
		1109	Cβ-twist (15); Cδ1-asym rock (11)	1071 (w)		1106	Cα-Cβ (33); N−Cα-C (10)
		1066	Cα-Cβ (37); N−Cα (14); NH3-asym rock (8)				
				998 (sh)		1004	N−Cα-C (11); Cβ-twist (11); Cγ-Cδ2 (9); Cδ2-asym rock (8)
				984 (m)		980	Cα-C (17); N−Ca (10)
962 (s)		976	Cδ2-asym rock (20); Cγ-Cδ2 (16); Cγ-Cδ1 (12); Cδ1-asym rock (11)	955 (m)		973	Cδ2-asym rock (38); Cδ1-asym rock (14); Cγ-Cδ1 (12); Cγ-Cδ2 (8)
		969	Cδ2-asym rock (28); W9...O−C (13); Cβ-Cγ (12)				
		965	Cδ1-asym rock (8)				
		959	Cβ-Cγ (15); Cδ1-asym rock (14)			959	Cβ-Cγ (26); Cδ1-asym rock (20); Cγ-Cδ2 (12); Cδ2-asym rock (8)
921 (sh)		939	Cδ1-asym rock(37); Cδ2-asym rock (21); Cγ-Cδ2 (9)	927 (w)		940	Cδ1-asym rock (40); Cδ2-asym rock (29)
905 (m)		904	Cα-C (17); W7...W8 (13); W8...NH3 (10); OCO (9)				
				851 (m)	854 (w)	867	Cβ-wag (26); ND3-asym rock (10)
852 (s)		853	Cβ-wag (19); N−Cα (12)			855	ND3-asym rock (20); Cα-Cβ (11)
830 (m)		827	Cγ-Cδ1 (17)	834 (m)	833 (w)	829	Cγ-Cδ1 (27); ND3-asym rock (15); Cβ-Cγ (12); Cγ-Cδ2 (11)
752 (m)		795	N−Cα-C (27); W10...O−C (26)	811 (m)	811 (w)	815	N−Cα (24); Cβ-wag (17); OCO (12)
				797 (m)		773	ND3-asym rock (31); W8...O−C (21); N−Cα-C (20); W10...O−C (13); N−Cα (12); W8...O−C (9); τ(N−Cα) (9)
				738 (m)		723	W8...O−C (15); W7...W8 (10); W5...W7 (9)
				702 (w)		684	W9...O−C (29); W9...W10 (14); W2...W5 (8)

[a] s. intense, m. medium, w. weak, sh. shoulder. Raman: vibrational wavenumbers in Raman spectra recorded in H_2O and D_2O buffers (see Figure 3). IR.: vibrational wavenumbers observed in FT−IR ATR spectra recorded in H_2O and D_2O (Figure 3). Calc: calculated results obtained at DFT/B3LYP/6-31++G* the level on a theoretical model including leucine surrounded by12 water molecules (Figure 4). Only major contributions (PED ≥ 8%) are reported in this Table. Assignments are based on the potential energy distribution (PED). In front of each internal coordinate is reported the corresponding PED (in percent).

energies ($E_v = 1/2 \sum h\nu$, where h is the Plank constant and ν the frequency of a vibrational mode) for each supermolecule. In the same table are the main geometrical parameters, such as bond length and valence angles for AAs as well as for water molecules, and additionally, the H-bond lengths related to the water molecules interacting with the NH_3^+ and COO^- charged groups of each AA. The calculated vibrational wavenumbers located in the 1800−700 cm^{-1} spectral range, arising mainly from amino acids, are reported in Tables 2 and 3 for comparison with the observed Raman and IR peaks.

V. Discussion

As Table 1 shows, the change in the chemical structure of the side chains only affects the geometrical parameters (bond lengths and valence angles) of atoms located in the vicinity of C_α. In addition, this change does not considerably perturb the whole H-bond network structure (W···W and W···AA) around AAs. This is principally due to the fact that all water molecules were basically located around the backbone of AAs, and also to the hydrophobic character (not hydrated) of the L side chain. On the basis of the present calculations, it can also be confirmed that the geometrical parameters of water molecules (bond lengths and valence angles) are not considerably affected by the chemical composition of the two studied amino acids. From the vibrational point of view, the comparison between the observed and calculated results can be undertaken through three spectral regions, as follows:

1750−1500 cm^{-1} Spectral Region. Thanks to the existence of intense IR bands, the vibrational modes arising from NH_3^+ angular bending and COO^- out-of-phase stretching motions can be appreciated (Tables 2 and 3). NH_3^+ bending modes observed at ca. 1640 cm^{-1} and 1510 cm^{-1} in IR spectrum completely disappear upon H−D isotopic substitution. Moreover, the calculations show that the NH_3^+ bending modes are considerably coupled with those of surrounding water molecules through W...AA hydrogen bonds. The same consideration explains that the COO^- asymmetric stretching mode observed at ca. 1600 cm^{-1} in both AAs in H_2O buffer, is shifted to higher wavenumbers in heavy water and give rise to intense and narrow IR bands at ca. 1615 cm^{-1} (Figures 2 and 3).

1500−1200 cm^{-1} Spectral Region. Both Raman and IR spectra give rise to intense bands in this region. Apart vibrational modes arising from COO^- in-phase stretching and NH_3^+ angular bending motions, this region provides very useful information on the side chain vibrational modes of CH_2 and CH_3 groups in leucine. The calculations allow us to assign the leucine modes observed in the 1450−1300 cm^{-1} spectral region to the HCH and CCH angular bendings, centered on the C_β, C_γ, $C_{\delta 1}$, and $C_{\delta 2}$ atoms of its side chain (Table 3), showing small isotopic shifts upon deuteration.

Below 1200 cm^{-1}. In this spectral region, deuteration leads somehow to a rearrangement of the vibrational modes (from skeletal origin in G, mainly from the side chain in L). The main vibrational modes of glycine are observed at 1033 and 898 cm^{-1} (Figure 2) are both assigned to the vibrational motions located around C_α atom. Both of them are considerably affected by deuteration (1033 → 1001 cm^{-1}; 898 → 837 cm^{-1}) because of the H−D replacement in the NH_3^+ group in one hand, and of the tight interaction of the COO^- group with its surrounding water (heavy water) molecules. An interesting effect in this region is the emergence of an intense mode at 966 cm^{-1} in Raman spectrum of deuterated glycine (Figure 2). This fact is interpreted by the coupling of the COO^- symmetric stretch motion with those corresponding to the $C-C_\alpha$ and $N-C_\alpha$ bonds. Like in the previous spectral region (1500−1200 cm^{-1}), leucine presents here a more complex vibrational scheme in comparison with glycine (Figure 3). The reason behind this fact can be explained as before: the more complex structure of the leucine side chain compared to that of glycine. The presence of explicit solvent around amino acids in the theoretical model considered in the present work allows us to appreciate, in many cases (Tables 2 and 3), the contribution of water molecules to the observed vibrational modes. Particularly, we can notice the modes with low intensity observed at 997 and 980 cm^{-1} in the Raman spectrum of glycine (Figure 2) which are mainly assigned to the intermolecular motions of W···AA and W···W types.

In conclusion, the present calculations lead us to conclude that terminal $NH3^+$ and COO^- groups of both amino acids might be, *in average*, fully hydrated in aqueous solution. This conclusion confirms the results obtained theoretically by recent CPMD calculations on hydrated glycine.[24]

VI. Concluding Remarks

This report presents a complete series of experimental results on vibrational features of glycine and leucine. As the side chain of both amino acids contain nonexchangeable hydrogens upon deuteration in heavy water, all isotopic shifts observed in vibrational spectra should mainly arise from the H−D substitution at the N-terminal of AAs and their interaction with surrounding heavy water. To propose reasonable assignments to the observed vibrational spectra, quantum mechanical calculations at the DFT/B3LYP/6-31++G* level of theory were performed on a cluster containing 12 water molecules surrounding the backbone of each amino acid. However, we are conscious that the calculated results based on the resolution of the time-independent Schrödinger equation, give only a static picture of hydration with fixed water molecules H-bonded to amino acids. The present models should thus be considered as a first step in investigating the dynamic hydration scheme of AAs in hydrated media. Acceptable assignments for vibrational spectra, along with reasonable isotopic shifts upon deuteration lead us now to consider quantum mechanical dynamics calculations on the hydrated AAs and peptides.

Acknowledgment. This work was performed thanks to a cooperation involving the Laboratoire de Spectroscopie Atomique Moléculaire et Applications (LASMA, Faculty of Science, EL MANAR University, Tunisia), the Department of Physics (University of Ngaoundere, Cameroon), and the Laboratoire de Biophysique Moléculaire, Cellulaire and Tissulaire (BioMoceTi, University Paris 13, France). We thank the Agence Universitaire pour la Francophonie (AUF) for the financial support to the scientific project (ref 6313PS567) established for a 2 year period 2005−2006, encouraging the mobility of Tunisian, Cameroonian, and French researchers. We also acknowledge two French supercomputer centers: IDRIS (Orsay, France) and CINES (Montpellier, France) for the computational time allocated to this project on IBM workstation networks.

References and Notes

(1) Xu, S.; Nilles, J. M.; Bowen, K. H., Jr. *J. Chem. Phys.* **2003**, *119*, 10696−10701.

(2) Clementi, E.; Cavallone, F.; Scordamaglia, R. *J. Am. Chem. Soc.* **1977**, *99*, 5531−5545.

(3) Császár, A. G. *J. Mol. Struct.* **1995**, *346*, 141−152.

(4) Stepanian, S. G.; Reva, I. D.; Radchenko, E. D.; Rosado, M. T. S.; Duarte, M. L. T. S.; Faust, R.; Adamowicz, L. *J. Phys. Chem. A* **1998**, *102*, 1041−1054.

(5) Pacios, L. F.; Gálvez, O.; Gómez, P. C. *J. Phys. Chem. A* **2001**, *105*, 5235−5241.
(6) Pacios, L. F.; Gómez, P. C. *J. Comput. Chem.* **2001**, *22*, 702−716.
(7) Ding, Y.; Krogh-Jespersen, K. *J. Comput. Chem.* **1996**, *17*, 338−349.
(8) Kassab, E.; Langlet, J.; Evleth, E.; Akacem, Y. *J. Mol. Struct. (Theochem*) **2000**, *531*, 267−282.
(9) Selvarengan, P.; Kolandaivel, P. *J. Mol. Struct. (Theochem)* **2002**, *617*, 99−106.
(10) Wang, W.; Zheng, W.; Pu, X.; Wong, N. B.; Tian, A. *J. Mol. Struct. (Theochem)* **2002**, *618*, 127−132.
(11) Wang, W.; Pu, X.; Zheng, W.; Wong, N. B.; Tian, A. *J. Mol. Struct. (Theochem)* **2003**, *626*, 235−244.
(12) Ramaekers, J.; Pajak, J.; Lambie, B.; Maes, G. *J. Chem. Phys.* **2004**, *120*, 4182−4193.
(13) Balta, B.; Aviyente, V. *J. Comp. Chem.* **2003**, *24*, 1789−1802.
(14) Balta, B.; Aviyente, V. *J. Comp. Chem.* **2004**, *25*, 690−703.
(15) Leung, K.; Rempe, S. B. *J. Chem. Phys.* **2005**, *122*, 18405−18418.
(16) Overman, S. A.; Thomas, G. J., Jr. *Biochemistry* **1999**, *38*, 4018−4027.
(17) Aubrey, K. L.; Thomas, G. J., Jr. *Biophys. J.* **1991**, *60*, 1337−1349.
(18) Overman, S. A.; Thomas, G. J., Jr. *Biochemistry* **1995**, *34*, 5440−5451.
(19) Frisch, M. J.; Trucks, G. W.; Schlegel, H. B.; Scuseria, G. E.; Robb, M. A.; Cheeseman, J. R.; Montgomery, J. A., Jr.; Vreven, T.; Kudin, K. N.; Burant, J. C.; Millam, J. M.; Iyengar, S. S.; Tomasi, J.; Barone, V.; Mennucci, B.; Cossi, M.; Scalmani, G.; Rega, N.; Petersson, G. A.; Nakatsuji, H.; Hada, M.; Ehara, M.; Toyota, K.; Fukuda, R.; Hasegawa, J.; Ishida, M.; Nakajima, T.; Honda, Y.; Kitao, O.; Nakai, H.; Klene, M.; Li, X.; Knox, J. E.; Hratchian, H. P.; Cross, J. B.; Bakken, V.; Adamo, C.; Jaramillo, J.; Gomperts, R.; Stratmann, R. E.; Yazyev, O.; Austin, A. J.; Cammi, R.; Pomelli, C.; Ochterski, J. W.; Ayala, P. Y.; Morokuma, K.; Voth, G. A.; Salvador, P.; Dannenberg, J. J.; Zakrzewski, V. G.; Dapprich, S.; Daniels, A. D.; Strain, M. C.; Farkas, O.; Malick, D. K.; Rabuck, A. D.; Raghavachari, K.; Foresman, J. B.; Ortiz, J. V.; Cui, Q.; Baboul, A. G.; Clifford, S.; Cioslowski, J.; Stefanov, B. B.; Liu, G.; Liashenko, A.; Piskorz, P.; Komaromi, I.; Martin, R. L.; Fox, D. J.; Keith, T.; Al-Laham, M. A.; Peng, C. Y.; Nanayakkara, A.; Challacombe, M.; Gill, P. M. W.; Johnson, B.; Chen, W.; Wong, M. W.; Gonzalez, C.; Pople, J. A. *Gaussian 03*, revision C.02; Gaussian, Inc.: Wallingford, CT, 2004.
(20) Becke, A. D. *J. Chem. Phys.* **1993**, *98*, 5648−5652.
(21) Lee, C.; Yang, W.; Parr, R. G. *Phys. Rev. B* **1988**, *37*, 785−789.
(22) Gaigeot, M. P.; Ghomi, M. *J. Phys. Chem. B* **2001**, *105*, 5007−5017.
(23) Chuaudhai, A.; Sahu, P. K.; Lee, S. L. *J. Mol. Struct. (Theochem)* **2004**, *683*, 115−119.
(24) Stepanian, S. G.; Reva, I. D.; Radchenko, E. D.; Adamowicz, L. *J. Phys. Chem. A* **1998**, *102*, 4623−4629.
(25) Frimand, K.; Bohr, H.; Jalkanen, K. J.; Suhai, S. *Chem. Phys.* **2000**, *255*, 165−194.
(26) Lima, J. A., Jr.; Freire, P. T. C.; Lima, R. J. C.; Moreno, A. J. D.; Mendes Filho, J.; Melo, F. E. A. *J. Raman Spectrosc.* **2005**, *36*, 1076−1081.
(27) Stepanian, S. G., Reva, I. D.; Radchenko, E. D.; Adamowicz, L. *J. Phys. Chem. A* **1999**, *103*, 4404−4412.